

2

## 3 **Lognormal distribution of firing time and rate from a single neuron?**

4

5

6 Eszter A. Kish<sup>1</sup>, Claes-Göran Granqvist<sup>2</sup>, András Dér<sup>3</sup>, Laszlo B. Kish<sup>4,a</sup>

7

8 <sup>1</sup> *Center for Learning and Memory, The University of Texas at Austin, 1 University*  
9 *Station, Stop C7000, Austin, TX 78712-0805*

10

11 <sup>2</sup> *Department of Engineering Sciences, The Ångström Laboratory, Uppsala University, P.*  
12 *O. Box 534, SE-75121 Uppsala, Sweden*

13

14 <sup>3</sup> *Institute of Biophysics, Biological Research Centre of the Hungarian Academy of*  
15 *Sciences, Temesvári krt. 62, P.O.B. 521, Szeged, H-6701, Hungary*

16

17 <sup>4</sup> *Department of Electrical and Computer Engineering, Texas A&M University, College*  
18 *Station, TX 77843-3128, USA*

19

20

21 **Abstract.** Even a single neuron may be able to produce significant lognormal features in  
22 its firing statistics due to noise in the charging ion current. A mathematical scheme  
23 introduced in advanced nanotechnology is relevant for the analysis of this mechanism in  
24 the simplest case, the integrate-and-fire model with white noise in the charging ion  
25 current.

26

27

28 In a recent review [1] the wide occurrence of lognormal-like distributions in the structural  
29 organization parameters and the firing rate of neurons were surveyed and their assumed  
30 functionalities were explored. It was assumed that the lognormal distribution of firing  
31 rates is the consequence of the specially organized circuit connectivity and the high  
32 complexity of the nervous system.

---

<sup>a</sup> Corresponding author. Laszlokish@email.tamu.edu

33

34 The natural question emerges if the internal dynamics of single neurons is already able to  
35 produce a lognormal firing feature due to its inherent stochastic features.

36

37 At the first look, such assumption looks rather unconventional. For example, several  
38 works study stochastic resonance with additive Gaussian noise [2,3] *in the membrane*  
39 *potential*. Due to the level-crossing properties of Gaussian noises, such models obviously  
40 result in a distribution of firing rates with no long-tail but exponential cutoff.

41

42 Still, experimental observations of lognormal firing statistics on lower levels of  
43 hierarchical organizations [4] seem to justify the question. Below, we present a  
44 quantitative example how the combination of plausible statistical assumptions and the  
45 simplest neuron model can lead to the appearance of lognormal firing rate distribution on  
46 the level of single neurons.

47

48 One of the well-known mathematical ways that lognormal distribution is obtained is a  
49 random walk on an axis with logarithmic scale (geometric random walk) resulting a  
50 growing Gaussian distribution over the axis, which is (due to the exponential stretch)  
51 equivalent to a lognormal distribution on the linear scale. Relevant applications of this  
52 model are stochastic stone cracking with fixed mean cracking fraction or its inverse  
53 process via coagulation/aggregation of nanoparticles [5]; both models result in lognormal  
54 size distribution.

55

56 However, these old models cannot account for the lognormal distribution of nanoparticle  
57 sizes at advanced vapor based fabrication methods [6,7] where the growth is  
58 condensational (linear in time) and when coagulation/aggregation is avoided. The origin  
59 of lognormal distribution in such cases was explained by a lognormal residence time  
60 distribution in the growth zone (vapor zone) of nanoparticle fabrication. Proceeding  
61 through the zone with a Brownian motion superimposed on a constant drift velocity  
62 results in a lognormal-like residence time distribution whenever the drift is strong and the  
63 starting point of the zone has a reflecting boundary [6,7]. The discrete difference equation

64 describing the progression through the zone is given as:

65

$$66 \quad x(k) = x(k-1) + \delta + \zeta(k)\sqrt{D} \quad , \quad (1)$$

67

68 where  $k$  is discrete time (measured in computational steps);  $x(k)$  is the position  
69 coordinate of the growing particle,  $\delta$  is the drift velocity;  $\zeta(k)$  is a random number with  
70 Gaussian (or other fast-cut-off, such as uniform) distribution, zero mean value, and unity  
71 variance; and  $D$  is the diffusion coefficient, which is the mean-square of the velocity  
72 noise resulting in the random-walk component superimposed on the drift. When the  $\zeta(k)$   
73 random numbers are independent,  $\zeta(k)$  represents a band-limited white noise thus the  
74 resulting random walk component is a Brownian motion.

75

76 The motion described by Equation 1 begins at  $x(0) = x_0$  and the first-passage time to the  
77 other end  $x_{th}$  of the zone is a random variable  $k_{th}$ . When the  $x_{th} \leq x(k_{th})$  is first satisfied,  
78 the growth process stops and  $k_{th}$  is recorded thus  $k_{th}$  is the residence time in the growth  
79 zone, that is, time spent by the linear growth. Here the threshold coordinate is given as  
80  $x_{th} = x_0 + L$ , where  $L$  is the length of the growth zone. The starting point  $x_0$  is a  
81 reflecting boundary, that is, the  $x_0 \leq x(k)$  condition is enforced during the whole motion.

82 The condition of strong drift means that the drift is greater than the critical value  $\delta_0$ :

83

$$84 \quad 1 < \delta / \delta_0 \quad , \quad (2)$$

85

86 where the critical drift depends on the strength of the noise and the length of the zone:

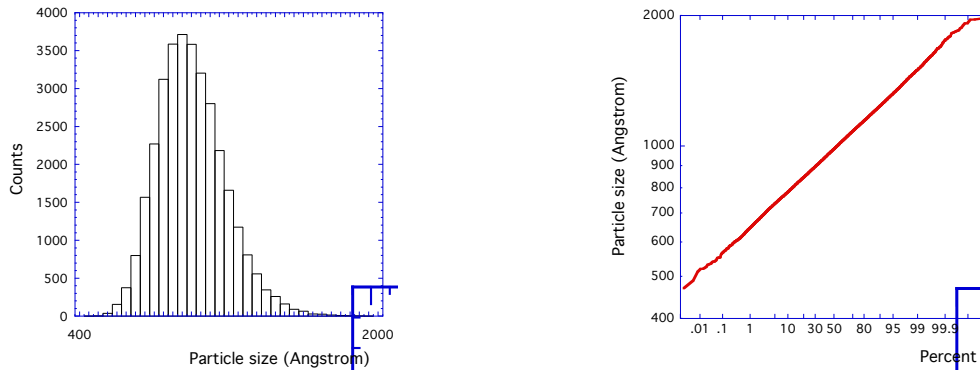
87

$$88 \quad \delta_0 = \frac{D}{L} \quad . \quad (3)$$

89

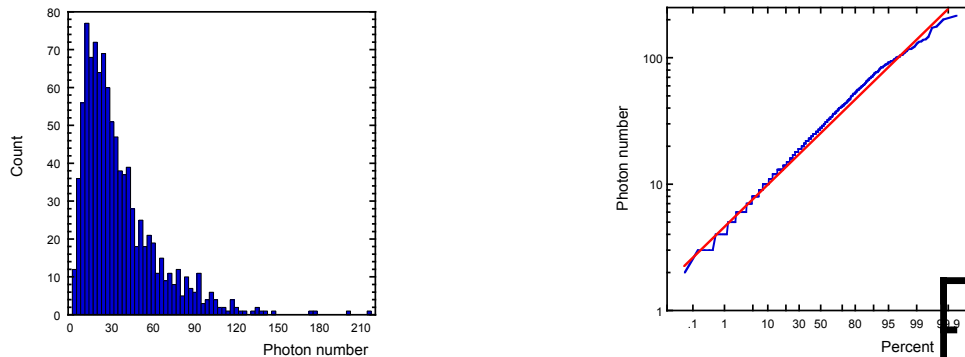
90 In the case of  $\delta = \delta_0$ , the noise-free drifting time through the system is equal to mean

91 first passage time due to the noise at zero drift. At strong drifts (Equation 2) the set  $\{k_{th}\}$   
 92 of residence time distribution is lognormal and, because the particle size is a linear  
 93 function of the residence time, lognormal particle size distribution is the result, see Figure  
 94 1.  
 95



96  
 97 **Figure 1.** Histogram of density size function (left), and cumulative distribution in log-Gaussian plot (right) of  
 98 the sizes of 100 thousand nanoparticles by condensational growth, without coagulation, due to Brownian  
 99 motion superimposed on linear drift in the growth zone (based on [6,7]). The log-Gaussian plot is much  
 100 more efficient than the histogram to follow the behavior in the long tail and a straight line represents ideal  
 101 lognormal distribution. Drift: 16.6 times the critical drift.  
 102

103 To explain the observed lognormality in the single protein molecule detection scheme  
 104 with fluorescent quantum dots, the same mathematical model was applied for quantum-  
 105 dot-marked-molecules drifting in a nanofluidic channel through a zone exposed to a laser  
 106 beam. Even the additional photonic shot noise could not destroy the lognormal feature in  
 107 the size distribution of photon bursts [8], see Figure 2.  
 108



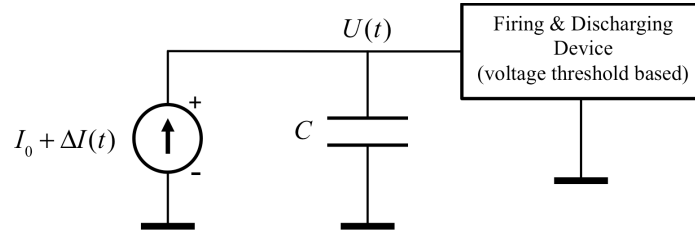
109

110 **Figure 2.** Histogram of density function (left), and cumulative distribution in log-Gaussian plot (right) of  
 111 photon burst sizes in single molecule detection with quantum dots [8]. Even the additional photon shot  
 112 noise in the model is unable to destroy the lognormal characteristic. Drift: 1.9 times the critical drift.

113

114 There is a striking similarity between the model described above and the integrate-and-  
 115 fire model, the simplest dynamical neuron model, if we suppose that there is a band-  
 116 limited white noise in the ion current, see Figure 3 for its circuit representation.

117



118

119

120 **Figure 3.** Circuit representation of the integrate-and-fire model: a capacitor is charged by a current  
 121 generator from the initial potential level  $U_0$  up to the threshold potential  $U_{th}$  where the firing takes place  
 122 and the capacitor is discharged. In the noise-free case, the membrane potential  $U(t)$  is drifting with  
 123  $\delta = I_0 / C$  velocity up to the firing threshold, where  $I_0$  is the charging ion current and  $C$  is the capacitance.  
 124 The current noise  $\Delta I(t)$ , when it is a band-limited white noise with Gaussian or other amplitude density of  
 125 fast cut-off, results in the sum of Brownian motion and a linearly drift in the membrane potential  $U(t)$ .  
 126 With a reflecting boundary at the initial potential value (or proper amplitude density of the noise to prohibit  
 127 backward propagation events) this is the same mathematical model as the one leading to Figure 1 (see  
 128 Equations 1-3).

129

130 Thus it is straightforward to apply the model as follows. In the discrete-time model, the  
 131 coordinate of the motion is the membrane potential  $U$ , the drift velocity of potential is  $\delta$ ,  
 132 and  $D$  is the mean-square of the noise in the ion current:

133

$$134 \quad U(k) = U(k-1) + \delta + \zeta(k)\sqrt{D} \quad , \quad (4)$$

135

136 where  $k$  and  $\zeta(k)$  are defined in the same way as in Equation 1. In accordance with

137 Equations 2 and 3, the critical drift is given as:

138

139 
$$\delta_0 = \frac{D}{U_{th} - U_0}, \quad (5)$$

140

141 where the initial potential value is  $U_0 = U(0)$  and the potential threshold of firing is  $U_{th}$ .

142 The starting point  $U_0$  is a reflecting boundary, that is, the  $x_0 \leq x(k)$  condition is enforced

143 during the whole process. When the  $U_{th} \leq U(k_{th})$  is first satisfied, the neuron fires, the

144 membrane potential is discharged and the whole charging process starts from the

145 beginning. The actual  $k_{th}$  value is recorded; it is the time interval between the former and

146 the present firing events (inter-spike interval). Here we assumed that the

147 firing/discharging process is negligibly short compared to the inter-spike interval.

148 because Equations 1 and 4 and the mathematical conditions are identical, in the strong

149 drift limit (see Equation 2), the set  $\{k_{th}\}$  has obviously lognormal distribution.

150 Furthermore, because any power function of a lognormally distributed random variable is

151 also lognormal, not only the inter-spike intervals but also the firing frequency will have

152 lognormal-like distribution if the firing/discharging process is negligibly short compared

153 to the inter-spike interval.

154

155 Figure 4 shows the histogram obtained by computer simulations of the integrate-and-fire

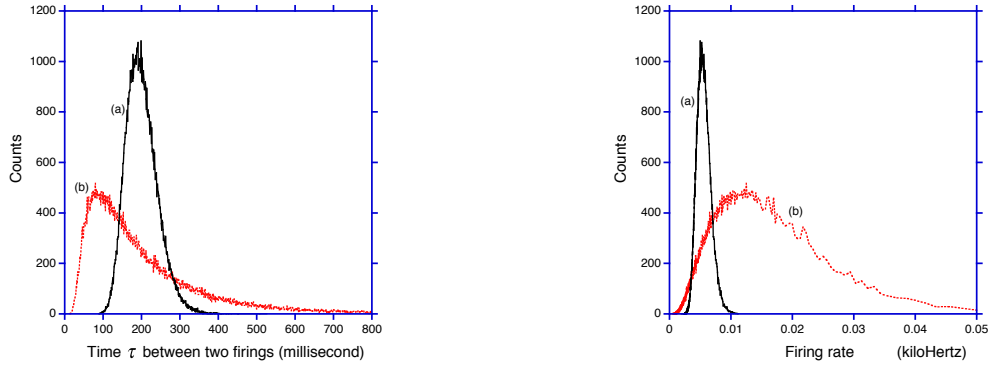
156 model with Equation 4 with  $U_0 = -60$  mV ,  $U_{th} = -40$  mV , and relative drifts

157  $\delta / \delta_0 = 6$  and  $24$  , respectively. Both the time and frequency data show the familiar

158 skewed shape.

159

160



161

162

163 **Figure 4.** Computer simulations of the integrate-and-fire model with white noise in the ion current causing  
 164 a random walk (Brownian motion) superimposed on the linear drift of the potential. The same random walk  
 165 model with special parameters used as in getting Fig. 1. The width and skewness of the resulting  
 166 lognormal-like distribution depend on the relative drift, which is the drift normalized to the critical drift  
 167 value. Because any power function of a lognormally distributed random variable has also lognormal  
 168 distribution, the lognormal distribution of time intervals between firing implies a lognormal distribution of  
 169 firing frequency (in the limit when the time spent for firing/discharging can be neglected). Drift (a) 6 times  
 170 and (b) 24 times the critical drift.

171

172 It is open question if the additive noise in the ion current is strong enough to yield the  
 173 observed distribution of firing frequency of single neurons. However, models and  
 174 observations [9] regarding the stochastic closing and opening of ion channels indicate  
 175 that the noise can be sufficiently strong. It is also an open question and subject of future  
 176 studies how much does the distribution deviate from lognormal in those cases when the  
 177 noise spectrum is  $1/f$  [10,11] instead of white and in the case of more advanced neuron  
 178 models.

179

180 Finally, we note that Longtin [12] studied stochastic resonance phenomena in the time  
 181 distribution of firing events at sinusoidal excitation of the Fitzhugh-Nagumo neuron  
 182 model. To introduce stochasticity, a white noise term was added to the time derivative of  
 183 the potential. In the case of no sinusoidal excitation, a skewed density function  
 184 (resembling lognormal) of the time intervals between firing events can be seen. However,  
 185 this fact was not commented because it was considered only as the base line of  
 186 observations and the paper was focusing on the induced periodicity and stochastic  
 187 resonance at sinusoidal driving in the presence of noise.

188

189

190 **Acknowledgements**

191

192 Discussions with Sergey Bezrukov (NIH) are appreciated.

193

194

195 **References**

196

- 197 1. G. Buzsaki and K. Mizuseki, "The log-dynamic brain: how skewed distributions  
198 affect network operations", *Nature Reviews Neuroscience* 15, 264-278 (2014).
- 199 2. S.M. Bezrukov and I. Vodyanoy, "Noise-induced enhancement of signal  
200 transduction across voltage-dependent ion channels", *Nature* 378, 362 - 364 (1995);  
201 doi:10.1038/378362a0.
- 202 3. Gingl, Kiss, Moss, "Non-dynamical stochastic resonance: Theory and experiments  
203 with white and arbitrarily coloured noise", *EPL (Europhysics Letters)* 29, 191-196  
204 (1995); doi:10.1209/0295-5075/29/3/001.
- 205 4. T. Hromadka, M.R. Dewese and A.M. Zador, "Sparse representation of sounds in  
206 the unanesthetized auditory cortex", *PLoS Biol.* 6, e16 (2008).
- 207 5. C.G. Granqvist and R.A. Buhrman, "Ultrafine metal particles", *J. Appl. Phys.* 47,  
208 2200 (1976).
- 209 6. J. Söderlund, L.B. Kiss, G.A. Niklasson, and C.G. Granqvist, "Lognormal Size  
210 Distributions in Particle Growth Processes without Coagulation", *Phys. Rev. Lett.*  
211 80, 2386 (1998).
- 212 7. L.B. Kiss, J. Söderlund, G.A. Niklasson and C.G. Granqvist, "New approach to the  
213 origin of lognormal size distribution of nanoparticles", *Nanotechnology* 10, 25-28,  
214 (1999).
- 215 8. L. L. Kish, J. Kameoka, C. G Granqvist, and L. B. Kish, "Log-Normal Distribution  
216 of Single Molecule Fluorescence Bursts in Micro/Nano-Fluidic Channels", *Appl.*  
217 *Phys. Lett.* 99 143121 (2011).
- 218 9. E.M. Nestorovich, V.A. Karginov, A.M. Berezhkovskii, V.A. Parsegian and S.M.

- 219 Bezrukov, "Kinetics and thermodynamics of binding reactions as exemplified by  
220 anthrax toxin channel blockage with a cationic cyclodextrin derivative", PNAS 109,  
221 18453-18458 (2012); doi: 10.1073/pnas.1208771109
- 222 10. S.M. Bezrukov, "The status of 1/f noise research in biological systems: Empirical  
223 picture and theories", in Proceedings of the First International Conference on  
224 Unsolved Problems of Noise, Szeged, 1996, edited by C.R. Doering, L.B. Kiss, and  
225 M.F. Schlesinger (World Scientific, Singapore, 1997), pp. 263–274.
- 226 11. Z. Siwy, A. Fulinski, "Origin of  $1/f^\alpha$  Noise in Membrane Channel Currents", Phys.  
227 Rev. Lett. 89, 158101 (2002); DOI: 10.1103/PhysRevLett.89.158101.
- 228 12. A. Longtin, "Stochastic Resonance in Neuron Models", J. Stat. Phys. 70, 309-327  
229 (1993).
- 230
- 231